ISME

ARTICLE

Demographic fluctuation of community-acquired antibiotic-resistant *Staphylococcus aureus* lineages: potential role of flimsy antibiotic exposure

Claude-Alexandre Gustave[1,2] · Anne Tristan[1,2] · Patricia Martins-Simões[1,2] · Marc Stegger[3] · Yvonne Benito[1,2] · Paal Skytt Andersen [3,4] · Michèle Bes[1,2] · Typhanie Le Hir[1,2] · Binh An Diep[5] · Anne-Catrin Uhlemann[6] · Philippe Glaser[7] · Frédéric Laurent[1,2] · Thierry Wirth[8,9] · François Vandenesch [1,2]

Abstract

Community-acquired (CA)- as opposed to hospital acquired- methicillin-resistant *Staphylococcus aureus* (MRSA) lineages arose worldwide during the 1990s. To determine which factors, including selective antibiotic pressure, govern the expansion of two major lineages of CA-MRSA, namely "USA300" in Northern America and "European ST80" in North Africa, Europe and Middle-East, we explored virulence factor expression, and fitness levels with or without antibiotics. The sampled strains were collected in a temporal window representing various steps of the epidemics, reflecting predicted changes in effective population size as inferred from whole-genome analysis. In addition to slight variations in virulence factor expression and biofilm production that might influence the ecological niches of theses lineages, competitive fitness experiments revealed that the biological cost of resistance to methicillin, fusidic acid and fluoroquinolones is totally reversed in the presence of trace amount of antibiotics. Our results suggest that low-level antibiotics exposure in human and animal environments contributed to the expansion of both European ST80 and USA300 lineages in community settings. This surge was likely driven by antibiotic (ab)use promoting the accumulation of antibiotics as environmental pollutants. The current results provide a novel link between effective population size increase of a pathogen and a selective advantage conferred by antibiotic resistance.

Introduction

Staphylococcus aureus remains one of the most common causative agents of both nosocomial and community-acquired infections. It colonizes asymptomatically at least $1/_3$ of humans and may cause infections with outcomes ranging from mild to life-threatening [1]. Until the mid-

✉ François Vandenesch
francois.vandenesch@univ-lyon1.fr

1 CIRI – Centre International de Recherche en Infectiologie, Inserm, U1111, Université Claude Bernard Lyon 1, CNRS, UMR5308, Ecole Normale Supérieure de Lyon, Univ Lyon, F-69007 Lyon, France

2 Centre National de Référence des Staphylocoques, Institut des Agents Infectieux, Hospices Civils de Lyon, Lyon, France

3 Department for Bacteria, Parasites and Fungi, Statens Serum Institut, Copenhagen, Denmark

4 Department of Veterinary and Animal Sciences, Frederiksberg, Denmark

5 Division of HIV, Infectious Diseases, and Global Medicine, Department of Medicine, University of California, San Francisco, CA, USA

6 Department of Medicine, Division of Infectious Diseases, Columbia University Medical Center, New York City, NY, USA

7 Institut Pasteur – APHP – Université Paris Sud, Unité Ecologie et Evolution de la Résistance aux Antibiotiques Paris, France, CNRS UMR3525 Paris, France

8 Institut de Systématique, Evolution, Biodiversité (ISYEB - UMR 7205, CNRS, MNHN, UPMC, EPHE), Muséum National d'Histoire Naturelle, Sorbonne Universités, Paris, France
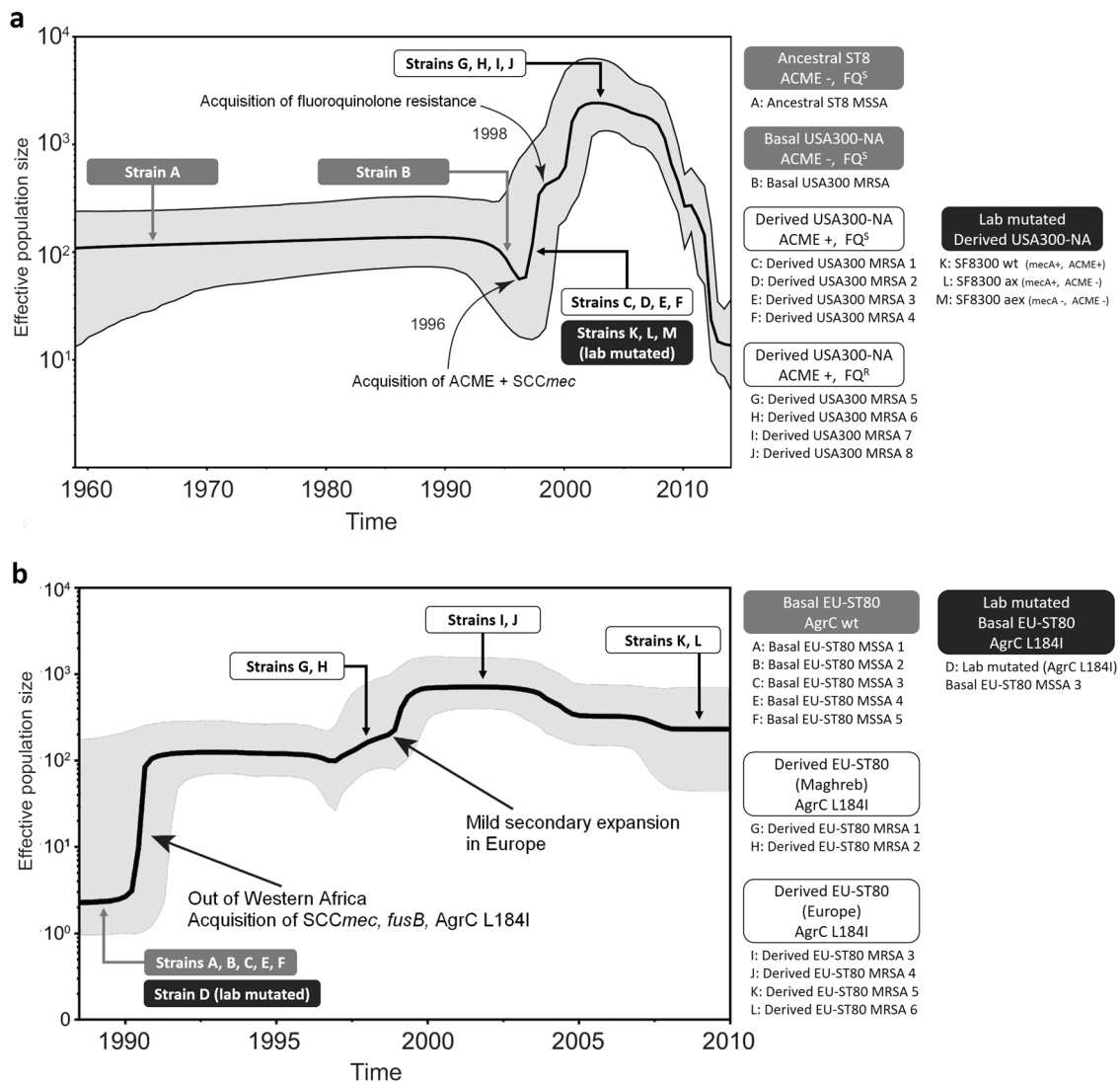
9 EPHE, PSL University, Paris, France

Fig. 1 Bayesian demography of USA300 and EU-ST80 lineages. Bayesian skyline plot indicating effective population size changes in the USA300 (**a**) and EU-ST80 (**b**) lineages over time with a relaxed molecular clock. Estimates of *S. aureus* effective number (Ne) through time are indicated on the *y*-axis, whereas calendar years are represented on the *x*-axis. The shaded area represents the 95% confidence interval. Strain selection and their designation are indicated by grey scale thumbnails (light grey = ancestral and basal clades; white = derived clade; dark grey = *in vitro* mutated strains). Adapted from Glaser *et al*. [12] and Stegger *et al*. [13]. FQ fluoroquinolones

1990s, methicillin-resistant *S. aureus* (MRSA) infections were reported almost exclusively from hospital settings and most hospital-associated MRSA (HA-MRSA) diseases resulted from a limited number of successful clones [2]. These HA-MRSA, which remained confined to healthcare settings, were exposed to a high-antibiotic pressure among patients with frequent immunity impairment and/or invasive devices, such as urinary/vascular catheters or mechanical ventilation [3]. Therefore, HA-MRSA was likely under strong positive selection within these healthcare-associated niches where acquisition of resistance to multiple antibiotic families provided them with a major competitive advantage despite their impaired fitness [4]. However, in early 2000s,

MRSA infections began to be reported in healthy individuals without known risk factors or apparent connections to healthcare institutions [5, 6]. These community-acquired (CA)-MRSA strains had genetic backgrounds distinct from the former HA-MRSA strains with specific lineages predominating in different continents such as the sequence type 8 (ST8) SCC*mec*IVa (standing for <u>s</u>taphylococcal <u>c</u>hromosomal <u>c</u>assette encoding <u>mec</u>hicillin resistance gene of type IVa) pulsotype USA300 in the USA (abbreviated to "USA300" below), the ST80 SCC*mec*IV in Europe, North Africa and Middle-East (hereinafter referred to as "EU-ST80"), and the ST30 SCC*mec*IV in Oceania [7]. Some genetic features of these CA-MRSA were postulated to be

Table 1 Relevant characteristics of strains

Strain designation (label in figures)	Ref. ID	Relevant characteristics	References
USA300 strains			
Ancestral ST8 MSSA (A)	ERS092996	*mecA*− ACME−, [*R* = *P*, *F*]	[17]
Basal USA300 MRSA (B)	ERS092816	*mecA*+, *ACME*−, [*R* = *P*, Oxa]	[17]
Derived USA300 MRSA 1 (C)	ST2012-0558	*mecA*+, ACME+, [*R* = *P*, Oxa]	[12]
Derived USA300 MRSA 2 (D)	ST2012-1514	*mecA*+, ACME+, [*R* = *P*, Oxa]	[12]
Derived USA300 MRSA 3 (E)	ST2013-0343	*mecA*+, ACME+, [*R* = *P*, Oxa, *K*, *E*]	[12]
Derived USA300 MRSA 4 (F)	ST2011-2484	*mecA*+, ACME+, [*R* = *P*, Oxa, *K*, *E*]	[12]
Derived USA300 MRSA 5 (G)	ST2011-1414	*mecA*+, ACME+, [*R* = *P*, Oxa, *K*, *E*, *O*]	[12]
Derived USA300 MRSA 6 (H)	ST2013-0068	*mecA*+, ACME+, [*R* = *P*, Oxa, *K*, *E*, *O*]	[12]
Derived USA300 MRSA 7 (I)	ST2013-1284	*mecA*+, ACME+, [*R* = *P*, Oxa, *K*, *E*, *O*, *T*]	[12]
Derived USA300 MRSA 8 (J)	ST2013-1763	*mecA*+, ACME+, [*R* = *P*, Oxa, *K*, *E*, *O*, *T*]	[12]
SF8300wt (K)	LUG2295 USA300 ref strain	*mecA*+, ACME+, [*R* = *P*, Oxa, *E*, *C*, *T*, Cip, Mup]	[20]
SF8300ax (L)	LUG2977 ACME deletion mutant	*mecA*+, Δ-ACME, [*R* = *P*, Oxa, *E*, *C*, *T*, Cip, Mup]	[20]
SF8300aex (M)	LUG2979 ACME and SCC*mec* deletion mutant	Δ-SCC*mec*, Δ-ACME, [*R* = *P*, *E*, *C*, *T*, Cip, Mup]	[20]
EU-ST80 strains			
Basal EU-ST80 MSSA 1 (A)	HT2002-0042	*mecA*−, AgrC wt, [*R* = *P*]	[13]
Basal EU-ST80 MSSA 2 (B)	HT2006-0859	*mecA*−, AgrC wt, [*R* = *P*]	[13]
Basal EU-ST80 MSSA 3 (C)	HT2003-0006	*mecA*−, AgrC wt, [*R* = *P*, *T*]	[13]
Lab Mutated Basal EU-ST80 MSSA 3 (D)	LUG2417	*mecA*−, AgrC L184I, [*R* = *P*, *T*]	This study
Basal EU-ST80 MSSA 4 (E)	HT2004-1302	*mecA*−, AgrC wt, [*R* = *P*, *T*]	[13]
Basal EU-ST80 MSSA 5 (F)	HT2005-0374	*mecA*−, AgrC wt, [*R* = *P*, *T*]	[13]
Derived EU-ST80 MRSA 1 (G)	ST2007-1277	*mecA*+, AgrC L184I, [*R* = *P*, Oxa]	[13]
Derived EU-ST80 MRSA 2 (H)	ST2007-1273	*mecA*+, AgrC L184I, [*R* = *P*, Oxa]	[13]
Derived EU-ST80 MRSA 3 (I)	ST2005-0508	*mecA*+, AgrC L184I, [*R* = *P*, Oxa, *K*, *F*]	[13]
Derived EU-ST80 MRSA 4 (J)	ST2009-0942	*mecA*+, AgrC L184I, [*R* = *P*, Oxa, *K*, *F*, *T*]	[13]
Derived EU-ST80 MRSA 5 (K)	HT2007-0258	*mecA*+, AgrC L184I, [*R* = *P*, Oxa, *K*, *F*, *T*, *E*, *C*]	[13]
Derived EU-ST80 MRSA 6 (L)	ST2007-1047	*mecA*+, AgrC L184I, [*R* = *P*, Oxa, *K*, *F*, *T*, *E*, *C*]	[13]

Strains list with their ID's (as used in the manuscript and figures), reference ID (as used in reference publications), relevant characteristics and reference publications

ACME arginine catabolism mobile element, *AgrC* accessory gene regulator, *C* clindamycin, *Cip* ciprofloxacin, *E* erythromycin, *F* fusidic acid, *I* isoleucine, *K* kanamycin, *L* leucine, *Mup* mupirocin, *O* ofloxacin, *Oxa* oxacillin, *P* penicillin, *R* resistant, *Ref. ID* strain designation used in reference articles, *SCC* Staphylococcal chromosomal cassette, *T* Tetracycline, *wt* wild-type

major determinants of their selective advantages against HA-MRSA in community settings [8]. Fitness impairment associated with the SCC*mec* mobile element is a well-described example: large SCC*mec* elements shared by HA-MRSA have higher fitness cost compared to small SCC*mec* of CA-MRSA [9]. Thus, under the lightened antibiotic pressure encountered outside healthcare settings HA-MRSA are outcompeted by CA-MRSA. Successful community spread of CA-MRSA has also been allegedly associated with ecological factors such as modifications of colonisation niches. This was illustrated by the hypothesis of a deleterious impact of anti-pneumococcal vaccines on nasal microbiota facilitating CA-MRSA colonization [10]. Finally, the observation that CA-MRSA have apparently increased virulence for human [11] notably in skin infection, suggests that higher bacterial load associated with increased severity of cutaneous infections could promote dissemination between humans.

Regarding the population dynamics of CA-MRSA, recent phylogenetic studies, conducted on the USA300 [12]

and the EU-ST80 [13] lineages, proposed two Bayesian evolutionary models inferring their population size through time among hundreds of isolates sampled from 1980s to 2000s. Those phylogenetic analyses strongly suggested that in the transition from an MSSA lineage to a successful CA-MRSA clone, the USA300 lineage first became resistant to multiple antibiotics, acquired the arginine catabolic mobile element (ACME), which encodes factors promoting skin colonization and infection [14, 15], and subsequently acquired resistance to fluoroquinolones [16, 17]. These two steps were associated with two successive phases of sharp demographic expansion of what is known as the USA300 North American (NA) lineage as opposed to the Latin-American variant (LV) which does not harbour ACME [12]. This evolutionary scenario has been confirmed recently on an independent set of strains revealing, in addition, the European origin of the USA300 ancestor [18]. A similar study, performed on the EU-ST80 epidemic CA-MRSA lineage, depicted a clone derived from a Panton-Valentine leucocidin (PVL)-positive methicillin-susceptible *S. aureus* (MSSA) ancestor from sub-Saharan Africa that dramatically expanded in the early 1990s once out of West Africa, upon acquisition of the SCC*mec* element, the plasmid-encoded fusidic acid resistance (*fus*B) and four canonical SNPs, including a non-synonymous mutation in the accessory gene regulator C (*agrC*) [13], a major virulence regulator in *S. aureus* [19]. However, for both the USA300 and the EU-ST80 lineages it remains to be demonstrated that the identified genetic events, which correlate with the demographic expansion, are causally related with population size variations. In order to answer these questions, we explored fitness and virulence factor expression of strains selected at various evolutionary and temporal stages of the predicted population size inferred through Bayesian coalescence models.

Materials and methods

Strain selection

Infection-related strain selection among the CA-MRSA clones USA300 and EU-ST80 was carried out based on three previously published phylogenetic studies [17, 12, 13]. All isolates were stored on cryobeads at −20 °C at the National Reference Center for Staphylococci (NRCS - HCL, Lyon). Prior whole-genome sequencing and Bayesian analysis of all strains enabled their assignment to an evolution phase of these lineages; thus isolates of the two lineages were selected at various temporal steps of their inferred population dynamics. For the CA-MRSA USA300 lineage and ancestors, 10 clinical isolates and three isogenic mutants were included (Fig. 1a and Table 1): (i) one

ancestral strain of the ST8 lineage, susceptible to methicillin and lacking ACME (Ancestral ST8 MSSA), (ii) one strain corresponding to the most recent common ancestor of the USA300 clone, being resistant to methicillin but lacking the ACME sequence (Basal USA300 MRSA), (iii) four strains from the early expansion phase characterized by ACME and SCC*mec* acquisition (Derived USA300 MRSA 1, 2, 3 and 4), (iv) four strains from the most recent evolutionary phase subsequent to fluoroquinolones resistance acquisition (Derived USA300 MRSA 5, 6, 7 and 8), as well as an USA300 reference strain (SF8300wt), its ACME single-deletion mutant (SF8300ax) and ACME-SCC*mec* double-deletion mutant (SF8300aex), both previously constructed by allelic replacement [20]. For the EU-ST80 lineage, eleven clinical isolates and one isogenic *agrC* mutant were selected (Fig. 1b and Table 1): (i) five strains from the basal clade with a high genetic proximity with their hypothetical Sub-Saharan Western Africa ancestor (Basal EU-ST80 MSSA 1, 2, 3, 4 and 5), (ii) two MRSA strains from the derived clade isolated on patients from Maghreb (Derived EU-ST80 MRSA 1 and 2), (iii) two MRSA strains from the derived clade isolated on patients from Europe (Derived EU-ST80 MRSA 3 and 4), (iv) two MRSA strains from the derived clade and associated with the stabilization/decline phase of the lineage (Derived EU-ST80 MRSA 5 and 6).

Construction of an EU-ST80 *agrC* mutant

The *agrC* locus of one basal MSSA of the ST80 lineage (Basal EU-ST80 MSSA 3) (Fig. 1b and Table 1) was mutated by allelic replacement to confer the sequence carried by isolates of the derived clade (isoleucine instead of leucine at position 184). This mutation was obtained by using pMAD [21]. Two *agrC* DNA fragments flanking the *agrC* target region were amplified from a wild-type strain using *agr*C2912/*agr*C555 and *agr*C544/*agr*C4238 primers, respectively (Table S2). DNA fragments were then blunt-ended by *Sca*I and *Pvu*II restriction enzymes, before being ligated and amplified using external primers *agr*C2912/*agr*C4238. The resulting DNA fragment corresponding to an *agrC* encoding sequence for the mutated amino acid I184 was restricted by *Xho*I and *Pvu*II and cloned into pMAD linearized by *Sal*I and *Sma*I. The resulting plasmid, pLUG1166, was electroporated into RN4220, and then into isolate Basal EU-ST80 MSSA 3. Transformants were grown at non-permissive temperature (42 °C), to select for cells with chromosome-integrated plasmid by homologous recombination. Successful double crossover mutants were subsequently selected on X-gal agar plates after single-colony culture at 30 °C for 10 generations. PCR amplifications and sequencing were used to confirm the mutation of *agrC* in the resulting strain

LUG2417 designated "Lab mutated basal EU-ST80 MSSA 3" (Table 1).

RNA extraction from *S. aureus*

Brain Heart Infusion (BHI) broth was inoculated with an overnight culture to an initial $OD_{600\,nm}$ of 0.05 and grown up on aerated Erlenmeyer flask to the end of exponential phase (6 h) at 37 °C under agitation (200 r.p.m.). One millilitre of bacterial suspension was harvested and concentration adjusted to an $OD_{600\,nm}$ of 1.0. Bacteria were washed in 10 mM Tris-buffer and treated with lysostaphin and β-mercaptoethanol. RNAs were extracted with the RNeasy Plus Mini Kit® (Qiagen), quantified by spectrophotometry and stored at −80 °C. This process was repeated on three different days for biological replicates.

RNA quantification by real-time PCR

A random-primers based reverse transcription of 1 µg of RNA was performed with the A3500 Reverse Transcription System Kit (Promega), followed by quantitative real-time PCR on cDNA using the FastStart Essential DNA Green Master kit (Roche) and the LightCycler® Nano (Roche). As previously described [11], we targeted five virulence genes (*RNAIII, lukS-PV, hla, hlgC* and *psmα*) and the house-keeping gene *gyrB* for normalization. Gene expression levels were compared between our clinical isolates; levels were expressed as n-fold differences relative to the most basal isolate of the strain set. These qRT-PCR's were performed as technical triplicates (three RNA quantification per RNA sample), on RNA obtained from three biological replicates (three independent cultures and extractions per strain).

Biofilm production assay

Each isolate was incubated overnight on blood agar (Columbia) at 35 °C under ambient air. Three colonies were transferred into 9 mL of BHI and incubated with agitation (200 r.p.m.) overnight at 35 °C under ambient air. Bacterial suspensions were then placed in a 96-well plate and incubated at 35 °C under ambient air for 24 h and 48 h, respectively. Biofilm production was assessed by spectrophotometry after well drying and crystal violet fixation. *S. aureus* laboratory strain SH1000 (a frequently used biofilm-producing control for *in vitro* biofilm models) was added as a positive control [22, 23], *Staphylococcus epidermidis* ATCC12228 (a biofilm-negative strain) [24] and *Staphylococcus carnosus* TM300 (a biofilm-negative strain lacking the *ica* gene and thus unable of intercellular adhesion) [25] were added as negative controls. Biofilm

experiments were performed as technical replicates (three wells per strain) and biological replicates (three independent plate series).

MIC determination

In order to adjust their concentrations in selective media and broth used for sub-inhibitory antibiotic pressure, minimal inhibitory concentration (MIC) of second line antibiotics were measured by E-tests® (bioMérieux) on Mueller-Hinton agar, and interpreted according to EUCAST specifications (EUCAST/CA-SFM v2.0, 2015 July).

Crude doubling time

Isolates growth curves were determined from BHI cultures incubated in 96-well plates for 24 h at 37 °C with continuous optical density monitoring at 600 nm (Tecan Infinite® 200 PRO). Each strain was inoculated in three independent wells (technical replicate), and the experiment was repeated on three different days (biological replicate). Doubling times were calculated by graphical method with the log-transformed optical density data of the exponential growth phase.

Competitive fitness

Each strain to be tested in a competitive pair was adjusted to an $OD_{600\,nm}$ of 1, then three mL of a $^1/_{100}$ dilution in BHI of each strain was mixed in a glass tube. For some experiments ofloxacin, ceftriaxone or fusidic acid were added at final concentrations corresponding to ¼ to $^1/_{100}$ of the susceptible strain's MIC. Tubes were incubated at 35 °C in aerobic atmosphere under agitation (200 r.p.m.) for 22±2 h, and 50 µL were transferred daily for 21 days to a fresh tube containing three mL of BHI. The proportion of each strain in the competitive mix was monitored at day 0, 3, 5, 10, 15 and 21 with differential colony count based on selective agar inoculated with a calibrated amount of competitive mix (Spiral System® - Interscience) followed by aerobic incubation for 24 h at 37 °C. For MSSA vs MRSA pairs, we used the ChromAgar® medium (i2A, France) allowing for growth of both strains (total count) and the ChromID-MRSA® medium (bioMérieux) for MRSA colony count. For the USA300 clone, we also used second line antibiotics resistance for strain discrimination. Therefore, differential colony counts were performed with simultaneous inoculation of a brain-heart agar (BHA) and a BHA with ofloxacin (2 µg/mL, i.e., five times above sensitive strain MIC, six times below resistant strain MIC). Similarly, for MRSA vs MRSA pairs belonging to the EU-ST80 lineage, a combination of BHA and BHA with tetracycline (1 µg/mL, eight times above sensitive strain MIC, eight times below
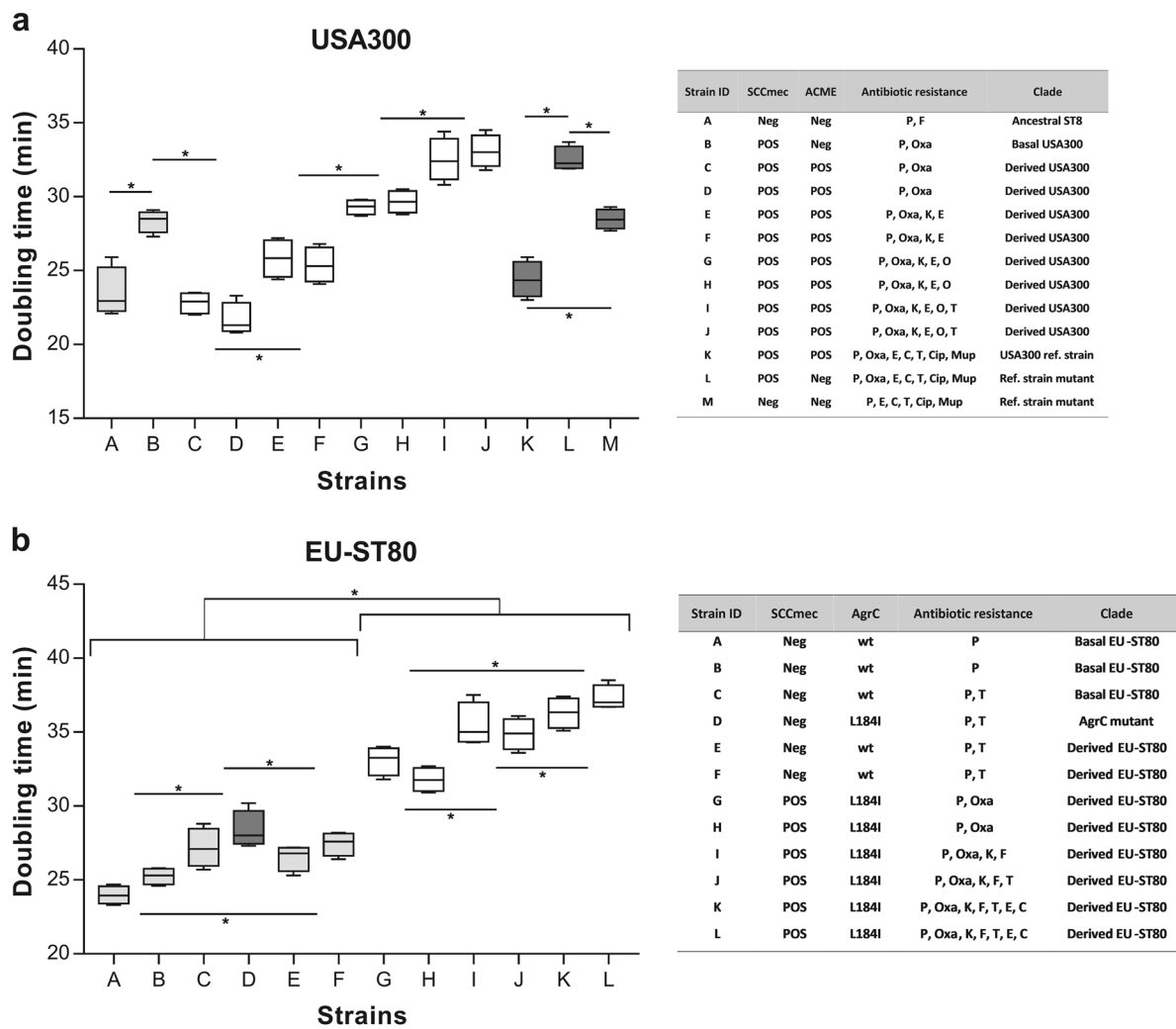
a

USA300

Strain ID	SCCmec	ACME	Antibiotic resistance	Clade
A	Neg	Neg	P, F	Ancestral ST8
B	POS	Neg	P, Oxa	Basal USA300
C	POS	POS	P, Oxa	Derived USA300
D	POS	POS	P, Oxa	Derived USA300
E	POS	POS	P, Oxa, K, E	Derived USA300
F	POS	POS	P, Oxa, K, E	Derived USA300
G	POS	POS	P, Oxa, K, E, O	Derived USA300
H	POS	POS	P, Oxa, K, E, O	Derived USA300
I	POS	POS	P, Oxa, K, E, O, T	Derived USA300
J	POS	POS	P, Oxa, K, E, O, T	Derived USA300
K	POS	POS	P, Oxa, E, C, T, Cip, Mup	USA300 ref. strain
L	POS	Neg	P, Oxa, E, C, T, Cip, Mup	Ref. strain mutant
M	Neg	Neg	P, E, C, T, Cip, Mup	Ref. strain mutant

b

EU-ST80

Strain ID	SCCmec	AgrC	Antibiotic resistance	Clade
A	Neg	wt	P	Basal EU-ST80
B	Neg	wt	P	Basal EU-ST80
C	Neg	wt	P, T	Basal EU-ST80
D	Neg	L184I	P, T	AgrC mutant
E	Neg	wt	P, T	Derived EU-ST80
F	Neg	wt	P, T	Derived EU-ST80
G	POS	L184I	P, Oxa	Derived EU-ST80
H	POS	L184I	P, Oxa	Derived EU-ST80
I	POS	L184I	P, Oxa, K, F	Derived EU-ST80
J	POS	L184I	P, Oxa, K, F, T	Derived EU-ST80
K	POS	L184I	P, Oxa, K, F, T, E, C	Derived EU-ST80
L	POS	L184I	P, Oxa, K, F, T, E, C	Derived EU-ST80

Fig. 2 Doubling times of USA300 and EU-ST80 strains. USA300 (**a**) or EU-ST80 (**b**) isolates as designated in Fig. 1 and Table 1, were cultured in BHI incubated on 96-wells plates for 24 h at 37 °C with continuous optical density monitoring at 600 nm (Tecan Infinite® 200 PRO). Doubling times were calculated by graphical method after Log transformation of data from the exponential growth phase. (*P = 0.029). Experiments were performed on three independent series (biological replicates), and optical densities were measured on three wells for each strain (technical replicates). Boxplots represent median and min to max replicates values. Light grey = ancestral ST8, basal USA300 and basal EU-ST80 clades; white = derived USA300 and derived EU-ST80 clades; dark grey = *in vitro* mutated strains

resistant strain MIC) was used. Strain quantifications calculated from colony counts on selective agar were confirmed by quantitative PCR targeting discriminant genes (*mecA* for MSSA vs. MRSA, *grlA* for fluoroquinolones sensitive vs. fluoroquinolones resistant, *tetK* for tetracycline sensitive vs. tetracycline resistant, or *arcA*-ACME for ACME negative vs. ACME-positive strains) carried by one of the strains in the competitive pair. This approach was used to rule out a growth inhibition bias on selective medium. This was also the only strain quantification method usable for the Basal EU-ST80 MSSA 3 in competition with its *agr*C derivative obtained by allelic replacement. Strain proportions were determined with a L184I-specific set of primers (Table S2). All the PCRs were performed at days 0,

3, 5, 10, 15 and 21. Continuous competitive cultures were performed on three independent series (biological triplicates); each colony count or qPCR was performed on three technical triplicates. For all strains pairs tested, one of the strains was eventually reduced to a trace level, so no statistical test was required for strain proportion comparisons.

Statistical analysis

Results are mostly presented as boxplots in figures and expressed as medians with 95% confidence interval (CI). Results from Figs. 2, 3 and 4 are presented in boxplots and expressed as medians with min/max range obtained from three technical replicates and three independent biological
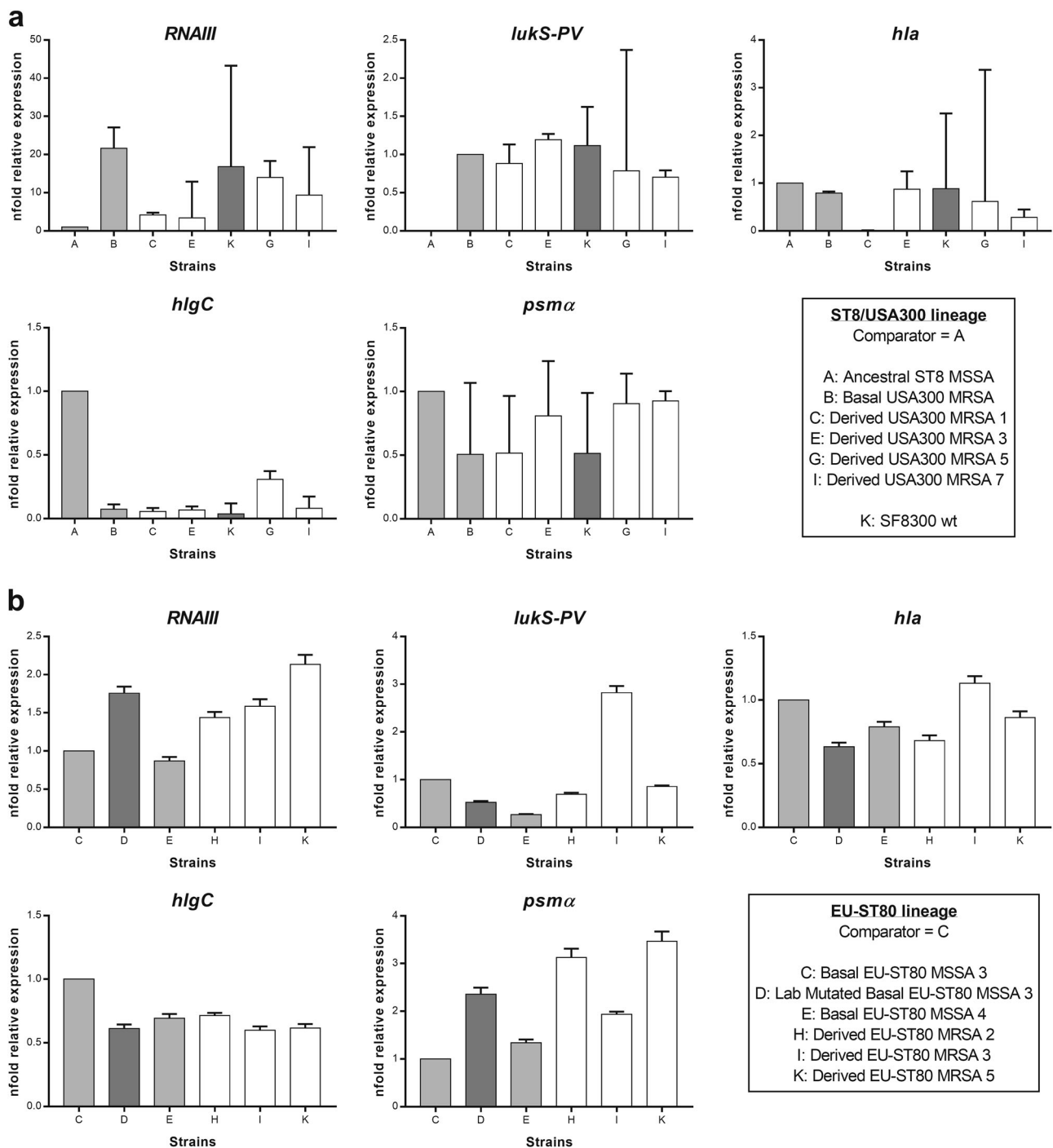
Fig. 3 Expression of virulence related genes among USA300 and EU-ST80 strains. Expression of virulence factor- and regulatory-genes were assessed by qRT-PCR among USA300 (**a**) and EU-ST80 (**b**) isolates designated as in Fig. 1 and Table 1. Light grey = ancestral ST8, basal USA300 and basal EU-ST80 clades; white = derived USA300 and derived EU-ST80 clades; dark grey = *in vitro* mutated strains. Results are expressed as fold change in comparison to the most basal strain of the lineage. Experiments were performed on three independent series (biological replicates), and three RNA quantifications were done for each RNA sample (technical replicates). Error bars represent 95% confidence interval. *In vitro* mutated strains are positioned among the other isolates according to their phylogenetic assignment

replicates. In Figs. 5, 6, 7 and 8, strains proportions in competitive pairs are presented as stacked histograms. All statistical comparisons were performed through non-parametric Mann–Whitney test (*P*-value <0.05). For competition experiments in which one strain was eventually reduced at undetectable level, no statistical test was required for proportion comparisons. All data were processed with Graphpad® PRISM 7.
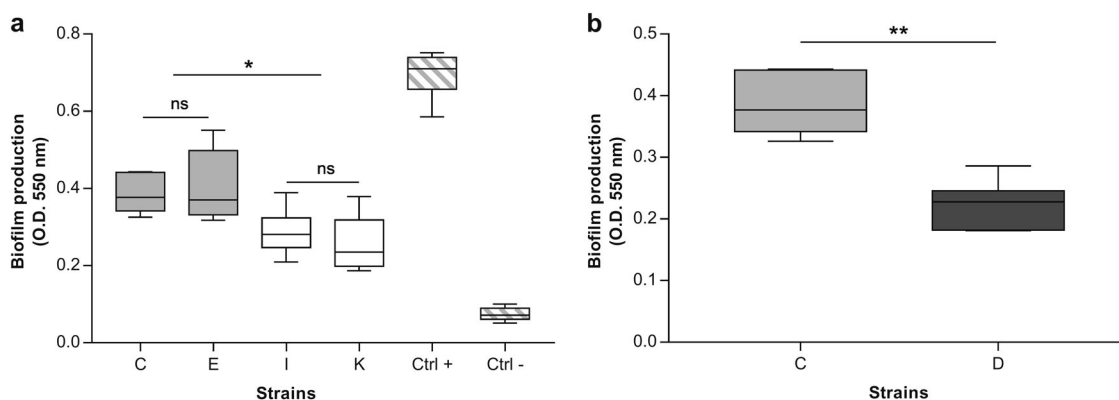
Fig. 4 Biofilm production assay for EU-ST80 strains. (a) Biofilm production was assessed by crystal violet stain on strains of the EU-ST80 lineage belonging to basal clade (strain C and E) or derived clade (strain I and K), the latter carrying the *mec*A gene and expressing an AgrC L184I variant. *S. aureus* SH1000 was used as positive control (ctrl+) for biofilm production and *S. carnosus* TM300 and *S. epidermidis* ATCC12228 were negative controls (ctrl−). (b) Comparison in biofilm production by crystal violet from a basal MSSA (strain C)

and its isogenic derivative expressing an AgrC L184I variant (strain D). All strains designation corresponds to those in Fig. 1 and Table 1. (*$P = 0.015$; **$P = 0.002$). Experiments were performed on three independent series (biological replicates), and biofilm production was quantified on three wells for each strain (technical replicates). Boxplots represent median and min to max replicates values. Light grey = basal EU-ST80 clade; white = derived EU-ST80 clades; dark grey = *in vitro* mutated strains; hatched boxes = controls

Results

Growth rate along the phylogeny

Previous studies showed that CA-MRSA grew significantly faster than HA-MRSA, a property that may be a prerequisite for CA-MRSA, in the absence of antibiotic pressure, to achieve successful colonization of humans by outcompeting the numerous bacterial species in the human environment outside the hospital setting [4]. We thus tested whether growth rate assessed by doubling-time varied between isolates of USA300 and EU-ST80 CA-MRSA lineages selected at various temporal steps of their Bayesian demography (Fig. 1 and Table 1). Whilst the ancestral ST8 MSSA strain (A) had short doubling time (~23.5 min), the basal USA300 MRSA isolate (B) carrying SCC*mec* had altered fitness with doubling time of ~28.4 min (Fig. 2a). In contrast, early-derived isolates of USA300 carrying both SCC*mec* and ACME (C and D) displayed shortened doubling time compared to the basal USA300 MRSA (B) (Fig. 2a). Within the derived clade corresponding to the epidemic phase, crude fitness appeared to be fading as we observed significant increase of doubling time along the phylogeny as shown by intraclade comparisons (Mann–Whitney test, $P = 0.029$ for all comparisons) (Fig. 2a). Each increase in doubling time appeared to be related to a new acquisition of antibiotics resistance, namely aminoglycosides and macrolides, then fluoroquinolones, followed by tetracyclines (Fig. 2a and Table 1). The opposite impact of SCC*mec* and ACME on doubling time was further confirmed by comparing the reference strain SF8300wt (strain K, phylogenetically close to strains E and F, see Fig. S1) with its ACME

deletion mutant (strain L), the later showing lengthened doubling time (Fig. 2a), whilst additional deletion of SCC*mec* (strain M, double ACME-SCC*mec* mutant) reduced the doubling time to an intermediate level (Fig. 2a). Among the twelve strains belonging to the EU-ST80 CA-MRSA lineage that were tested, the shortest doubling times were observed for the "basal clade" isolates (interclade comparison, Mann–Whitney test, $P = 0.029$) (Fig. 2b). Within each clade (basal and derived), we observed a decreasing crude fitness along the phylogeny as shown by increasing of doubling times (intraclade comparisons, Mann–Whitney test, $P = 0.029$ for all comparisons) (Fig. 2b). As for USA300 strains, antibiotics resistance appeared to be a major determining factor of doubling time lengthening as shown by interclade comparison (Basal MSSA vs Derived MRSA, Mann–Whitney test, $P = 0.029$), and by intraclade comparisons revealing longer doubling times associated with new acquisition of antibiotics resistance, namely tetracyclines within the basal clade of MSSA strains (strains C, E and F). In contrast, in the derived clade, fitness impairments resulted from the consecutive acquisition of resistance to methicillin, fusidic acid, aminoglycosides, and finally tetracyclines and macrolides for the most recent isolates (Mann–Whitney test, $P = 0.029$ for all comparisons) (Fig. 2b and Table 1). At this stage, as epidemic strains (from derived clades) displayed the longest doubling times, we concluded that crude *in vitro* fitness did not explain the evolutionary dynamic of the two lineages. We therefore investigated other features related to host interaction and antibiotic pressure that could explain the demography of both lineages.
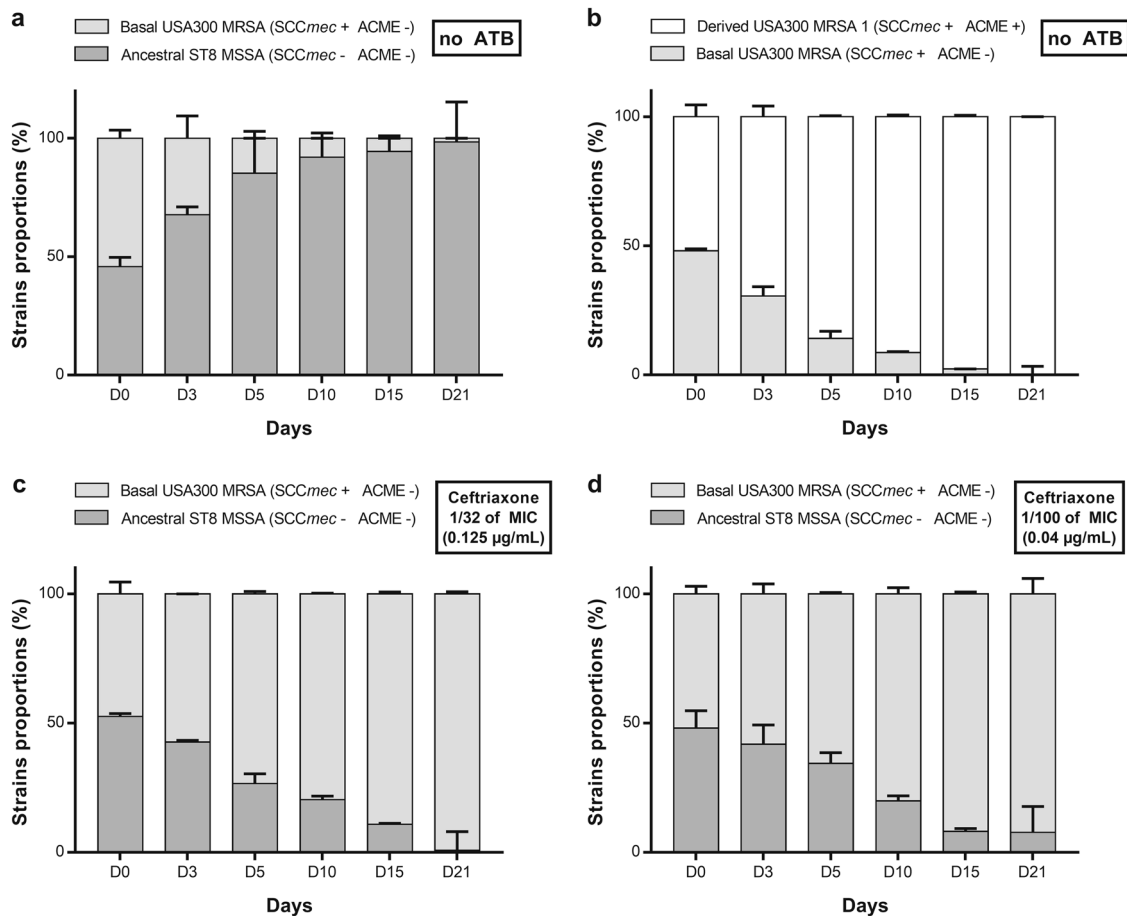
Fig. 5 Impact of *mec*A and ACME in competitive fitness of USA300. (**a**) Ancestral ST8 MSSA and Basal USA300 MRSA both ACME-negative were co-cultivated for 21 days in BHI with daily subculture in fresh medium without antibiotics, or (**c**) containing ceftriaxone at $^{1}/_{32}$ of ceftriaxone MIC of the susceptible strain (0.125 μg/mL), or (**d**) $^{1}/_{100}$ MIC (0.04 μg/mL). (**b**) Basal USA300 MRSA and derived USA300 MRSA 1 were co-cultivated for 21 days in BHI with daily subculture in fresh medium without antibiotic. The proportion of each strain was monitored at day 0, 3, 5, 10, 15 and 21 with qPCR targeting *mec*A (**a**, **b**, **c**) or *arc*A-ACME (**d**). Competitive cultures were performed on three independent series (biological replicates), and each colony count or qPCR was repeated three times (technical replicates). Error bars represent 95% confidence interval. Light grey = ancestral ST8, basal USA300 clades; white = derived USA300 clade

Expression of core-genome encoded virulence factors along the lineages' evolutionary history

Previous studies revealed that overexpression of core-genome encoded virulence factors was a common feature of CA-MRSA, a characteristic that has been proposed to contribute to the expansion of these lineages [11]. We therefore tested whether variations in the expression of core genome encoded virulence factors along the Bayesian demographic models could be observed (Fig. 1). To this end, qRT-PCRs targeting virulence factors of the core- (α-toxin, PSMα, γ-toxin) and accessory-genome (*lukS-PV*), as well as the major regulator (*agr*-RNAIII), were performed after *in vitro* post-exponential growth as previously described [11]. Within the ST8/USA300 lineage, the comparison between the ancestral ST8 MSSA isolate (A) and the Basal USA300 MRSA strain (B) revealed several

important variations in gene expression including a 15-fold increase in RNAIII (the *agr*-related regulatory RNA), a twofold decrease in *hla*, a 10-fold decrease of *hlg*C and a twofold decrease in *psmα* (Fig. 3a). However, when considering the variation in expression along the phylogeny of the USA300 lineage (i.e., variations that could correlate with the two steps of demographic expansion), despite an outlier strain with no measurable expression of *hla*, and a twofold increase in RNAIII (threefold when including the reference strain SF8300) and *psmα*, no major variations were detected in expression levels of the targeted virulence factors between the strains representing the two steps of expansion (strains C, E, G, I) (Fig. 3a). For the EU-ST80 lineage, most of the targeted virulence factors studied showed variation in expression below - or close to - twofold, between ancestral and derived isolates with the exceptions of i) *psmα* increasing by 3–3.5-fold in two
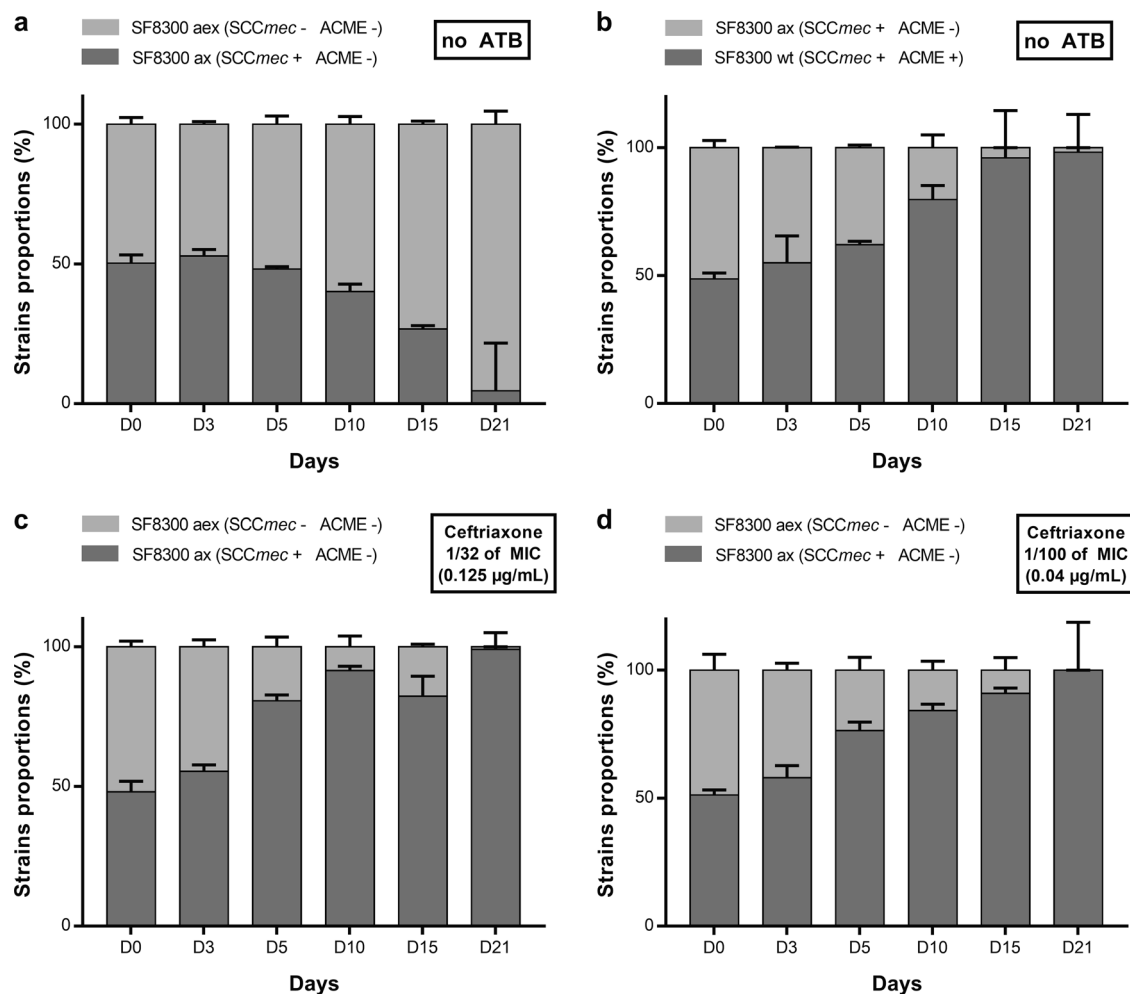
Fig. 6 Impact of *mec*A and ACME in competitive fitness of USA300 isogenic mutants. (**a**) SF8300 aex and SF8300 ax both ACME-negative were co-cultivated for 21 days in BHI with daily subculture in fresh medium without antibiotics, or (**c**) containing ceftriaxone at $^{1}/_{32}$ of ceftriaxone MIC of the susceptible strain (0.125 µg/mL), or (**d**) $^{1}/_{100}$ MIC (0.04 µg/mL). (**b**) SF8300 wt and SF8300 ax, both MRSA were co-cultivated for 21 days in BHI with daily subculture in fresh medium without antibiotic. The proportion of each strain was monitored at day 0, 3, 5, 10, 15 and 21 with qPCR targeting *mec*A (**a**, **b**, **c**) or *arcA*-ACME (**d**). Competitive cultures were performed on three independent series (biological replicates), and each colony count or qPCR was repeated three times (technical replicates). Error bars represent 95% confidence interval

isolates from the evolutionary-derived clade (strain H and K), and ii) *luk*S-PV increasing by a factor of 2.8-fold in one isolate (strain I) (Fig. 3b). In addition, as observed for the USA300 lineage, expression of RNAIII was slightly increased among isolates of the derived clade (reaching a 2.1-fold increase for one strain) compared to the basal clade (Fig. 3b).

All the EU-ST80 isolates from the derived clade harbour an L184I mutation in the extracellular loop of the AgrC receptor [13], a mutation that may have a functional impact on Agr signalling and expression of *agr*-RNAIII. To further investigate this point, an ancestral ST80 (AgrC wt) was engineered by allelic replacement to carry the L184I substitution and was then tested for quantification of RNAIII and virulence factor expression. Compared to wild-type (strain C), the mutated (L184I) isogenic derivative (strain

D) showed a slight enhancement of RNAIII expression, but below the level of 2 (Fig. 3b). This mutation had no significant impact on virulence gene expression, except a 2.2-fold increase in *psm*α expression (Fig. 3b).

Biofilm production

The detection of a slight difference in RNAIII production associated with the *agrC* mutation in the EU-ST80 lineage prompted us to test whether it could translate into differences in biofilm production. After 48 h of growth, basal MSSA 3 and 4 (strain C and E) displayed a higher production of biofilm compared to derived MRSA 3 and 5 (strain I and K) carrying the L184I AgrC substitution (*P* = 0.0002) (Fig. 4). The role of AgrC L184I substitution in this phenotypic difference was confirmed by comparing strain
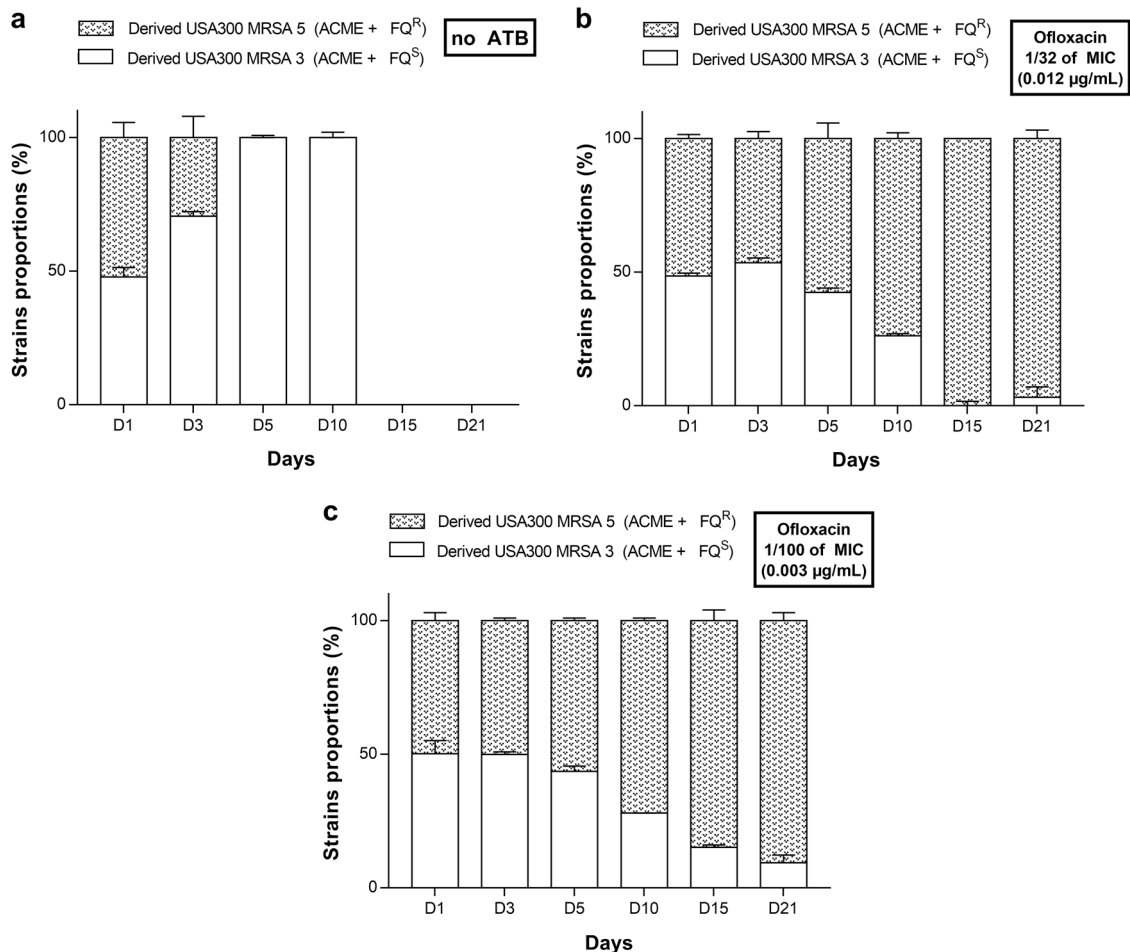
Fig. 7 Potential impact of FQ resistance in competitive fitness of USA300. (**a**) Fluoroquinolone (FQ)-susceptible derived USA300 MRSA 3 and FQ-resistant derived USA300 MRSA 5, both ACME-positive, were co-cultivated for 21 days in BHI without antibiotics, or (**b**) containing ofloxacin at $^1/_{32}$ of FQ MIC of the susceptible strain (0.012 μg/mL), or (**c**) $^1/_{100}$ MIC (0.003 μg/ml) with daily subculture in fresh medium. The proportion of each strain was monitored daily with differential colony count based on selective agar inoculated with a calibrated amount of competitive mix, and qPCR targeting *grlA at* day 0, 3, 5, 10, 15 and 21. Competitive cultures were performed on three independent series (biological replicates), and each colony count or qPCR was repeated three times (technical replicates). Error bars represent 95% confidence interval

C, the basal EU-ST80 MSSA 3 (AgrC wt) with its isogenic derivative, strain D (L184I), the latter showing a significant reduction of biofilm production ($P < 0.0001$). Importantly, the AgrC L184I mutation had no significant impact on crude fitness since doubling times of the mutated strain (D) and its wild-type parental strain (C) were similar (Fig. 2b). Therefore, differences observed in biofilm production were not due to growth variations but rather actual differences in biofilm production.

Competitive fitness along the phylogeny

Doubling times comparisons used for crude fitness assessment highlighted fitness modulations along the phylogeny that did not match the Bayesian models inferred for both lineages (Fig. 1). To better address this issue, we conducted a competitive fitness experiment in more stringent conditions based on continuous co-cultures for 21 days with isolates belonging to each phase of these lineages' evolution. Competitive strains pairs were designed in order to assess each evolutionary breakpoint identified in their inferred Bayesian coalescence models [12, 13], (Table 1 and S1). Moreover, since our assessment of crude doubling times identified the acquisition of antibiotics resistance as a major determinant of fitness alteration, we tested the impact of sub-inhibitory concentrations of antibiotics on competitive fitness of these isolates. Within the ST8/USA300 lineages, ancestral ST8 MSSA outcompeted the Basal USA300 MRSA (Fig. 5a) in the absence of antimicrobials, confirming the biological cost associated with the acquisition of the SCC*mec* element. The fitness compensation associated with ACME acquisition was confirmed in the competition experiment between Basal USA300 MRSA and derived USA300 MRSA 1 or 2 in which the later
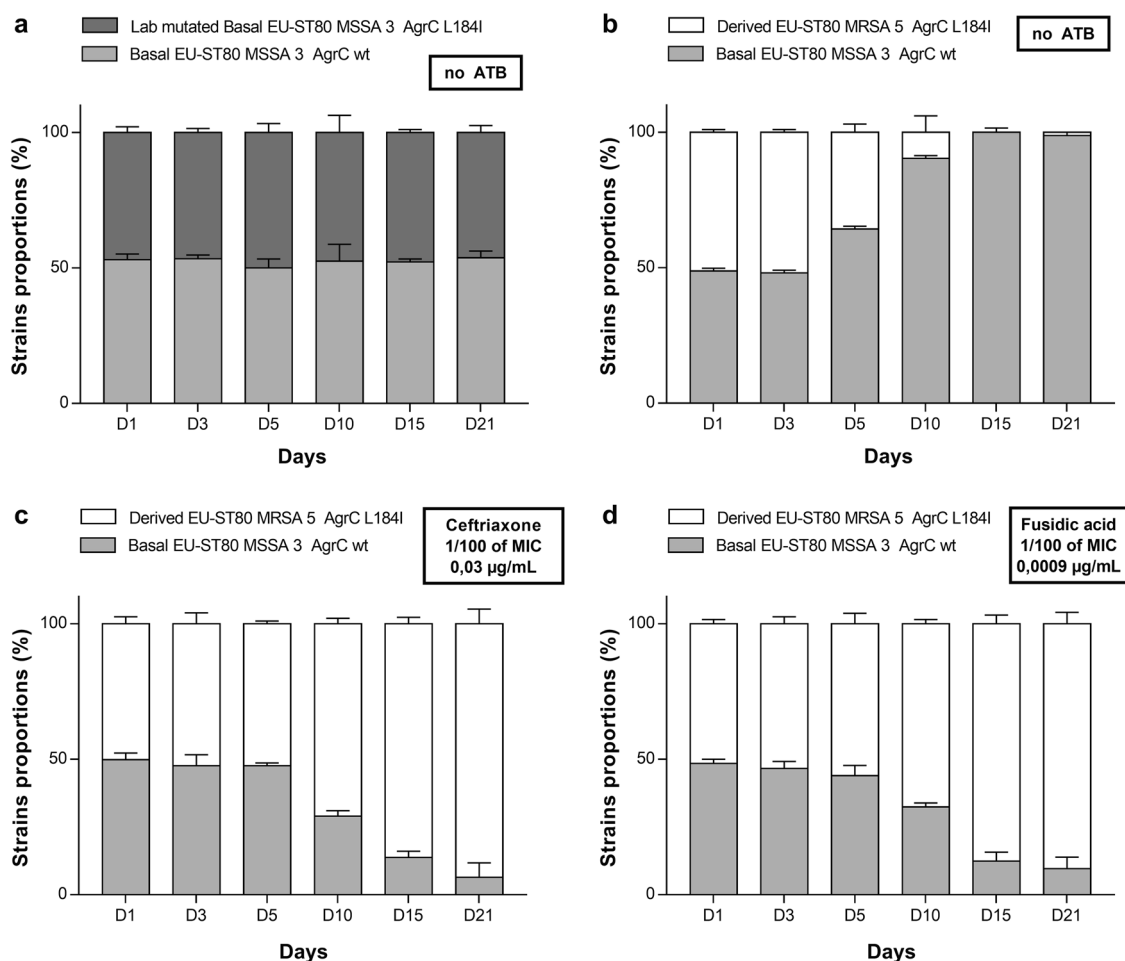
Fig. 8 Potential impact of *mecA/fusB* acquisition and *agrC* mutation on competitive fitness of EU-ST80. (**a**) Basal EU-ST80 MSSA 3, *agrC* wild-type was co-cultivated with its *agrC* derivative Lab mutated Basal EU-ST80 MSSA 3 carrying the AgrC L184I mutation. (**b**) Basal EU-ST80 MSSA 3, *agrC* wild-type and derived EU-ST80 MRSA 5 carrying the AgrC L184I mutation were co-cultivated for 21 days in BHI without antibiotics (**b**) or containing ceftriaxone (**c**) or fusidic acid (**d**) at $^1/_{100}$ of MIC for the MSSA (0.03 µg/mL or 0.0009 µg/mL respectively) with daily subculture in fresh medium. The proportion of each strain was monitored at day 0, 3, 5, 10, 15 and 21 with differential colony count based on selective agar inoculated with a calibrated amount of competitive mix for (**b, c, d**) or by qPCR due to the lack of discriminant antibiotic resistance marker for (**a**). The same results were obtained with antibiotics concentrations of $^1/_{16}$ and $^1/_{32}$ of their MICs (data not shown). Competitive cultures were performed on three independent series (biological replicates), and each colony count or qPCR was repeated three times (technical replicates). Error bars represent 95% confidence interval. Light grey = basal EU-ST80 clade; white = derived EU-ST80 clade; dark grey = *in vitro* mutated strains

outcompeted the former (Fig. 5b and supplementary figure 2). Similar results were obtained by using the isogenic strains in competition: in the absence of ACME, the presence of SCC*mec* was deleterious as strain SF8300aex outcompeted strain SF8300ax (Fig. 6a), and in the presence of SCC*mec*, a functional ACME reversed the fitness as SF8300wt outcompeted SF8300ax (Fig. 6b). However, when considering the more recently derived clades of USA300, the fitness enhancement conferred by ACME acquisition was progressively abolished along the phylogeny with the acquisition of fluoroquinolone (FQ) resistance: FQ-resistant ACME-positive derived USA300 MRSA 5 was outcompeted in only a few days by FQ-susceptible ACME-positive derived USA300 MRSA 3

(Fig. 7a). The same results were obtained during competition between the FQ-resistant derived USA300 MRSA 5 and another FQ-susceptible isolate (derived USA300 MRSA 4) (supplementary figure 3a). After FQ resistance was acquired, competitive fitness dropped even below the level observed prior to ACME acquisition, as FQ-resistant derived USA300 MRSA 5 and 6 appeared less fit than the FQ-sensitive ACME negative basal USA300 MRSA (supplementary figure 4a and b, respectively). Altogether these results indicate that ACME enhances fitness but is insufficient to compensate for the fitness cost of FQ resistance.

To assess whether the fitness cost of resistance could be reversed in the presence of trace amounts of antibiotics that are potentially present in the environment [4, 26],

competitive cultures were performed at various sub-inhibitory concentrations of antibiotics. The antibiotics chosen were those for which resistance acquisition correlate with noticeable variation in effective population size of the lineages (beta-lactams, fusidic acid for EU-ST80, and beta-lactams, fluoroquinolones for USA300). For USA300, low concentration of beta-lactam ($^1/_{100}$ of MSSA Ceftriaxone MIC, 0.04 µg/mL) was sufficient to confer a strong selective advantage both when testing either clinical isolates (Ancestral ST8 MSSA vs Basal USA300 MRSA (Fig. 5c, d); Ancestral ST8 MRSA vs Derived USA300 MRSA 1, supplementary figure 5 b and c), or isogenic strains (SF8300ax vs SF8300aex, Fig. 6c, d). In the derived clade that became resistant to fluoroquinolones, even extremely low-FQ concentration ($^1/_{100}$ of the FQ-susceptible strain's MIC, 0.0038 µg/mL) conferred a strong selective advantage of FQ-resistant ACME-positive strain toward FQ-susceptible ACME-positive strain (Fig. 7b, c; supplementary Fig. 3b and c) or toward FQ-susceptible ACME-negative strain (supplementary Fig. 4b and d). Similar analyses performed on the EU-ST80 strains also confirmed the results obtained during doubling times assessment, suggesting that the major factor ruling the fitness downfall along the phylogeny was not the AgrC L184I but the acquisition of SCCmec/fusB and further extended antibiotics resistance. In competitive culture assays, the laboratory engineered agrC mutation did not translate into fitness impairment after 21 days of competitive culture with its wild-type progenitor (Fig. 8a). However, competitive culture of the clinical strains confirmed the strong fitness reduction of the derived EU-ST80 MRSA isolates compared to the basal EU-ST80 MSSA in favour of a fitness cost of antibiotics acquisition (the most premature being SCCmec and fusB) in the absence of antibiotics (Fig. 8b). Similar results were obtained with Basal EU-ST80 MSSA 4 vs. Derived EU-ST80 MRSA 3 (supplementary figure 6a). The same competition performed in the presence of sub-inhibitory concentration of beta-lactam or fusidic acid reversed the result with a strong advantage of the MRSA even at extremely low-concentrations ($^1/_{100}$ of MSSA Ceftriaxone MIC, 0.03 µg/mL, and $^1/_{100}$ of MSSA fusidic acid MIC, 0.0009 µg/mL) (Fig. 8c, d). Similar results were obtained when applying these antibiotics concentrations on the pair Basal EU-ST80 MSSA 4 vs. Derived EU-ST80 MRSA 3 (supplementary figure 6b and c).

Discussion

Polyphyletic CA-MRSA emergence and spread at the end of the 20th century [6, 27], remains a challenging issue. As pointed out before, "our understanding of how a clone [such as USA300 or EU-ST80] became established as an endemic pathogen within communities remains limited" [17]. Increased expression of core-genome encoded virulence factors has been shown to be a common feature of CA-MRSA [11]. We have investigated whether such characteristics varied along the longitudinal short-term evolution of CA-MRSA. However, by assessing transcription of virulence factors previously described as over-expressed among CA-MRSA lineages [11], we could detect only modest variations (ca. between 2 and 3-fold) in RNAIII (the agr-related regulatory RNA)- and for some isolates in PSMα-expression between basal and derived isolates of both USA300 and EU-ST80 lineages (Fig. 3). We cannot rule out however that, at the population level, these minor increases in virulence factor expression enhanced the success of the lineage, for instance by increasing cutaneous infection rate. These represent the most common infections caused by S. aureus and thus may accelerate human-to-human transmission by skin contact as observed in prisons, sport team or men having sex with men [28].

Our current study indicates that alternative factors contribute to the fitness of USA300. We previously showed, that within the USA300 clone, 20 SNPs were identified for being under positive selection along successful evolution of this lineage [12]; however, all the derived isolates assessed for doubling time carried these 20 SNPs. Therefore, despite being under positive selection they could not be reliable determinants of crude fitness evolution of the derived clade isolates as competitive fitness impairment observed along the phylogeny would not be explained by these genetic variations. Thus, the major variable feature of USA300 along the demography was the acquisition of ACME which is a now well-characterized mobile genetic element (MGE) acquired from S. epidermidis by horizontal gene transfer [29, 30, 17]. ACME harbours multiple functions in resistance to acidic pH which enhances skin colonization, and as a factor promoting resistance to skin innate-immune defences [2]. Combined, these features make it a very plausible contributor of the USA300 expansion [31]. This is further strengthened by our findings of a shorter doubling-time of strains carrying ACME (Fig. 2a) both, when comparing strains along the phylogeny (such as strain B lacking ACME and strains C and D that carry it) and laboratory deletion mutants of ACME (SF8300 and derivatives) (Fig. 2a). In the case of EU-ST80, previous analyses of the strains included in the present study showed that isolates of the basal and derived clades of this lineage were discriminated by four canonical SNPs [13]. One was located in a non-coding region, two were synonymous SNPs, and one was a non-synonymous SNP located in agrC, the major virulence factor regulator involved in quorum sensing and biofilm production. We focused our attention on this SNP

located in the *agrC* gene, because of its potential association to fitness and colonization ability. This SNP resulted in a L184I amino acid change in the extracellular loop of the AgrC receptor [13] shared by all EU-ST80 isolates belonging to the derived clade. To investigate this point further, an ancestral ST80 (AgrC wt) was engineered by allelic replacement to carry the L184I substitution. Despite a slight increase of doubling time compared to its parental strain, the L184I change in AgrC did not translate into significant crude fitness variation (Mann–Whitney test, *P* = 0.343). Assessment of virulence factor expression revealed a twofold increase of *psmα* in the *in vitro* mutated strain compared to its parental wild-type progenitor (Fig. 3b). AgrC L184I could therefore have a moderate impact on virulence. We further detected a strong and significant decrease in biofilm production associated with the AgrC L184I mutation (Fig. 4). Assessing which of these phenotypes (slight increase in PSMα or PVL, strong decrease in biofilm) was under selection remains speculative because they could be strongly dependent on the ecosystem in which selection has occurred. However, little is known regarding these ecological conditions since the current model for CA-MRSA ST80 lineage expansion places the acquisition of the AgrC L184I mutation in the early 1990s in strains originating from Sub-Saharan Western Africa, concomitantly with the acquisition of SCC*mec*IV and *fusB* [13]. Alternatively, the AgrC L184I substitution might be neutral, belonging to canonical mutations following the acquisition of SCC*mec*IV and *fusB* or a consequence of genetic drift. Importantly, antibiotic resistance was associated with demographic expansion of both, EU-ST80 (acquisition of SCC*mec*IV and *fusB*) and North American USA300 (acquisition of SCC*mec* and fluoroquinolone resistance) (Fig. 1) [13, 12]. The acquisition of each of these resistance determinants was associated with a significant fitness cost as indicated by both extended doubling-time of the derived isolates (Fig. 2) and in the competition experiments where derived isolates were outcompeted by their basal counterparts (Figs. 5–8 and Supplementary figures 2–6). These observations were in accordance with the classical fitness costs associated with *de novo* antibiotic resistance, specifically those selected at high-antibiotic concentration [32, 33]. Conversely, they did not match the Bayesian evolutionary models of these lineages, as strains belonging to the epidemic phase (derived clade) displayed the lowest *in vitro* competitive fitness, with each step of fitness decrease being associated with new acquisition of antibiotic resistance (Fig. 2, Table 1). However, the most striking observation was that extremely low concentrations of antibiotics (those for which resistance acquisition correspond to demographic expansion of the two lineages) reversed this fitness cost. This is in line with recent demonstration of a close correspondence between the estimated growth rates of a MRSA

lineage and population-level prescription rates of beta-lactam antibiotics [34]. Since both USA300 and EU-ST80 likely emerged in low income populations [6, 32, 31] where antibiotic exposure was not believed to be substantial, the role of antibiotic selective pressure was not initially considered to be the major trait under positive selection. However, an increasing number of reports reveals the escalation of antibiotic as environmental pollutants originating from hospital wastewater, bulk drug producer wastewater and unused antibiotics dumped in landfills in countries without solid take-back programs [35, 36, 26, 37]. From these sources, in which antibiotics such as fluoroquinolones can reach concentrations ranging from 3 ng/L to 240 μg/L [38], antibiotics are disseminated in various environmental matrices, such as surface water, soil, sediments and eventually living organism including livestock [38]. Hence, community settings, even in remote populations, can be exposed to low-level concentrations of various antibiotics that could have promoted the expansion of CA-MRSA at least by enriching for resistant bacteria [33], if not selecting for *de novo* resistance, the latter being typically associated with no fitness cost [39, 33, 40]. Here we demonstrated with competition experiments—assuming the inherent limitations of the *in vitro* model—that the biological cost of antibiotic resistance (to beta-lactams, fusidic acid and fluoroquinolones) is entirely reversed in the presence of trace amounts of antibiotics. Previous studies based on multidrug-resistant plasmids showed that, for specific combinations of drugs, each new compound added, lowered the minimal selective concentration of the others [41]. However antibiotic resistance acquisitions (both by horizontal transfer of resistance genes and by mutations) are the genetic events that best match the variation of the demography in both lineages (Fig. 1). Altogether, our findings support a model of antibiotic use, misuse and pollution as a major driving force for the emergence and expansion of CA-MRSA. In conclusion, CA-MRSA dynamics appear to be ruled by a complex interplay between resistance, virulence and fitness cost in which the contribution of anthropogenic activities is substantial.

Compliance with ethical standards

References

1. Lowy FD. Staphylococcus aureus Infections. N Engl J Med. 1998;339:520–32.

2. Thurlow LR, Joshi GS, Richardson AR. Virulence strategies of the dominant USA300 lineage of community associated methicillin resistant *Staphylococcus aureus* (CA-MRSA). FEMS Immunol Med Microbiol. 2012;65:5–22.

3. Chavez TT, Decker CF. Health care-associated MRSA versus community-associated MRSA. Dis Mon. 2008;54:763–8.

4. Okuma K, Iwakawa K, Turnidge JD, Grubb WB, Bell JM, O'Brien FG, et al. Dissemination of new methicillin-resistant *Staphylococcus aureus* clones in the community. J Clin Microbiol. 2002;40:4289–94.

5. Chambers HF. The changing epidemiology of *Staphylococcus aureus*? Emerg Infect Dis. 2001;7:178–82.

6. Vandenesch F, Naimi T, Enright MC, Lina G, Nimmo GR, Heffernan H, et al. Community-acquired methicillin-resistant *Staphylococcus aureus* carrying Panton-Valentine Leukocidin genes: worldwide emergence. Emerg Infect Dis. 2003;9:978–84.

7. Mediavilla JR, Chen L, Mathema B, Kreiswirth BN. Global epidemiology of community-associated methicillin resistant *Staphylococcus aureus* (CA-MRSA). Curr Opin Microbiol. 2012;15:588–95.

8. David MZ, Daum RS. Community-associated methicillin-resistant *Staphylococcus aureus*: epidemiology and clinical consequences of an emerging epidemic. Clin Microbiol Rev. 2010;23:616–87.

9. Ma XX, Ito T, Tiensasitorn C, Jamklang M, Chongtrakool P, Boyle-Vavra S, et al. Novel type of staphylococcal cassette chromosome mec identified in community-acquired methicillin-resistant *Staphylococcus aureus* strains. Antimicrob Agents Chemother. 2002;46:1147–52.

10. Regev-Yochay G, Trzciński K, Thompson CM, Malley R, Lipsitch M. Interference between Streptococcus pneumoniae and *Staphylococcus aureus*: in vitro hydrogen peroxide-mediated killing by Streptococcus pneumoniae. J Bacteriol. 2006;188:4996–5001.

11. Li M, Cheung GYC, Hu J, Wang D, Joo H-S, DeLeo FR, et al. Comparative analysis of virulence and toxin expression of global community-associated methicillin-resistant *Staphylococcus aureus* Strains. J Infect Dis. 2010;202:1866–76.

12. Glaser P, Martins-Simões P, Villain A, Barbier M, Tristan A, Bouchier C, et al. Demography and intercontinental spread of the USA300 community-acquired methicillin-resistant *Staphylococcus aureus* lineage. mBio. 2016;7:e02183–15.

13. Stegger M, Wirth T, Andersen PS, Skov RL, De Grassi A, Simões PM, et al. Origin and evolution of European community-acquired methicillin-resistant *Staphylococcus aureus*. mBio. 2014;5: e01044–14.

14. Thurlow LR, Joshi GS, Clark JR, Spontak JS, Neely CJ, Maile R, et al. Functional modularity of the arginine catabolic mobile element contributes to the success of USA300 methicillin-resistant *Staphylococcus aureus*. Cell Host Microbe. 2013;13:100–7.

15. Planet PJ, LaRussa SJ, Dana A, Smith H, Xu A, Ryan C, et al. Emergence of the epidemic methicillin-resistant *Staphylococcus aureus* strain USA300 coincides with horizontal transfer of the arginine catabolic mobile element and speG-mediated adaptations for survival on skin. mBio. 2013;4:e00889–13.

16. Challagundla L, Luo X, Tickler IA, Didelot X, Coleman DC, Shore AC, et al. Range expansion and the origin of USA300 North American epidemic methicillin-resistant *Staphylococcus aureus*. mBio. 2018;9:e02016–17.

17. Uhlemann A-C, Dordel J, Knox JR, Raven KE, Parkhill J, Holden MTG, et al. Molecular tracing of the emergence, diversification, and transmission of S. aureus sequence type 8 in a New York community. Proc Natl Acad Sci USA. 2014;111:6738–43.

18. Strauß L, Stegger M, Akpaka PE, Alabi A, Breurec S, Coombs G, et al. Origin, evolution, and global transmission of community-acquired Staphylococcus aureus ST8. Proc Natl Acad Sci USA. 2017;114:E10596–E10604.

19. Reynolds J, Wigneshweraraj S. Molecular insights into the control of transcription initiation at the Staphylococcus aureus agr operon. J Mol Biol. 2011;412:862–81.

20. Diep BA, Stone GG, Basuino L, Graber CJ, Miller A, des Etages S-A, et al. The arginine catabolic mobile element and staphylococcal chromosomal cassette mec linkage: convergence of virulence and resistance in the USA300 clone of methicillin-resistant Staphylococcus aureus. J Infect Dis. 2008;197:1523–30.

21. Arnaud M, Chastanet A, Débarbouillé M. New vector for efficient allelic replacement in naturally nontransformable, low-GC-content, gram-positive bacteria. Appl Environ Microbiol. 2004;70:6887–91.

22. Horsburgh MJ, Aish JL, White IJ, Shaw L, Lithgow JK, Foster SJ. σB modulates virulence determinant expression and stress resistance: characterization of a functional rsbU strain derived from Staphylococcus aureus 8325-4. J Bacteriol. 2002;184:5457–67.

23. O'Neill Aj. Staphylococcus aureus SH1000 and 8325-4: comparative genome sequences of key laboratory strains in Staphylococcal research. Lett Appl Microbiol. 2010;51:358–61.

24. Zhang Y-Q, Ren S-X, Li H-L, Wang Y-X, Fu G, Yang J, et al. Genome-based analysis of virulence genes in a non-biofilm-forming Staphylococcus epidermidis strain (ATCC 12228). Mol Microbiol. 2003;49:1577–93.

25. Rosenstein R, Nerz C, Biswas L, Resch A, Raddatz G, Schuster SC, et al. Genome analysis of the meat starter culture bacterium Staphylococcus carnosus TM300. Appl Environ Microbiol. 2009;75:811–22.

26. Gothwal R, Shashidhar T. Antibiotic pollution in the environment: a review. CLEAN – Soil Air Water. 2015;43:479–89.

27. Tristan A, Bes M, Meugnier H, Lina G, Bozdogan B, Courvalin P, et al. Global distribution of panton-valentine leukocidin–positive methicillin-resistant *Staphylococcus aureus*, 2006. Emerg Infect Dis. 2007;13:594–600.

28. Diep BA, Chambers HF, Graber CJ, Szumowski JD, Miller LG, Han LL, et al. Emergence of multidrug-resistant, community-associated, methicillin-resistant *Staphylococcus aureus* clone USA300 in men who have sex with men. Ann Intern Med. 2008;148:249–57.

29. Diep BA, Gill SR, Chang RF, Phan TH, Chen JH, Davidson MG, et al. Complete genome sequence of USA300, an epidemic clone of community-acquired meticillin-resistant *Staphylococcus aureus*. Lancet. 2006;367:731–9.

30. Pi B, Yu M, Chen Y, Yu Y, Li L. Distribution of the ACME-arcA gene among meticillin-resistant Staphylococcus haemolyticus and identification of a novel ccr allotype in ACME-arcA-positive isolates. J Med Microbiol. 2009;58:731–6.

31. Planet PJ. Life after USA300: the rise and fall of a superbug. J Infect Dis. 2017;215:S71–S77.

32. Martinez JL. The role of natural environments in the evolution of resistance traits in pathogenic bacteria. Proc R Soc B Biol Sci. 2009;276:2521–30.

33. Andersson DI, Hughes D. Microbiological effects of sublethal levels of antibiotics. Nat Rev Microbiol. 2014;12:465–78.

34. Volz EM, Didelot X (2018). Modeling the growth and decline of pathogen effective population size provides insight into epidemic dynamics and drivers of antimicrobial resistance. *Syst Biol*. e-pub ahead of print, https://doi.org/10.1093/sysbio/syy007.

35. Naimi TS, LeDell KH, Como-Sabetti K, Borchardt SM, Boxrud DJ, Etienne J, et al. Comparison of community- and health care–associated methicillin-resistant *Staphylococcus aureus* infection. JAMA. 2003;290:2976–84.

36. Larsson DGJ. Antibiotics in the environment. Ups J Med Sci. 2014;119:108–12.

37. See I, Wesson P, Gualandi N, Dumyati G, Harrison LH, Lesher L, et al. Socioeconomic factors explain racial disparities in invasive community-associated methicillin-resistant *Staphylococcus aureus* disease rates. Clin Infect Dis. 2017;64:597–604.

38. Van Doorslaer X, Dewulf J, Van Langenhove H, Demeestere K. Fluoroquinolone antibiotics: an emerging class of environmental micropollutants. Sci Total Environ. 2014;500–501:250–69.

39. Gullberg E, Cao S, Berg OG, Ilbäck C, Sandegren L, Hughes D, et al. Selection of resistant bacteria at very low antibiotic concentrations. PLoS Pathog. 2011;7:e1002158.

40. Westhoff S, van Leeuwe TM, Qachach O, Zhang Z, van Wezel GP, Rozen DE. The evolution of no-cost resistance at sub-MIC concentrations of streptomycin in Streptomyces coelicolor. ISME J. 2017;11:1168–78.

41. Gullberg E, Albrecht LM, Karlsson C, Sandegren L, Andersson DI. Selection of a multidrug resistance plasmid by sublethal levels of antibiotics and heavy metals. mBio. 2014;5:e01918–14.